Title

Multiple interactions between an Arf/GEF complex and charged lipids determine activation kinetics on the membrane

Journal

Proceedings of the National Academy of Sciences of the United States of America, 114(43)

ISSN

0027-8424

Authors

Karandur, Deepti
Nawrotek, Agata
Kuriyan, John
et al.

Publication Date

2017-10-24

DOI

10.1073/pnas.1707970114

Peer reviewed

Multiple interactions between an Arf/GEF complex and charged lipids determine activation kinetics on the membrane

Deepti Karandur[a,b,1], Agata Nawrotek[c,d,1], John Kuriyan[a,b,2], and Jacqueline Cherfils[c,d,2]

[a]Department of Molecular and Cell Biology, University of California, Berkeley, CA 94720; [b]Howard Hughes Medical Institute, University of California, Berkeley, CA 94720; [c]Laboratoire de Biologie et Pharmacologie Appliquée, CNRS, Cachan 94235, France; and [d]Ecole Normale Supérieure Paris-Saclay, Cachan 94235, France

Edited by Satyajit Mayor, National Centre for Biological Sciences, Bangalore, India, and approved August 28, 2017 (received for review May 15, 2017)

Lipidated small GTPases and their regulators need to bind to membranes to propagate actions in the cell, but an integrated understanding of how the lipid bilayer exerts its effect has remained elusive. Here we focused on ADP ribosylation factor (Arf) GTPases, which orchestrate a variety of regulatory functions in lipid and membrane trafficking, and their activation by the guanine-nucleotide exchange factor (GEF) Brag2, which controls integrin endocytosis and cell adhesion and is impaired in cancer and developmental diseases. Biochemical and structural data are available that showed the exceptional efficiency of Arf activation by Brag2 on membranes. We determined the high-resolution crystal structure of unbound Brag2 containing the GEF (Sec7) and membrane-binding (pleckstrin homology) domains, revealing that it has a constitutively active conformation. We used this structure to analyze the interaction of uncomplexed Brag2 and of the myristoylated Arf1/Brag2 complex with a phosphatidylinositol bisphosphate (PIP_2) -containing lipid bilayer, using coarse-grained molecular dynamics. These simulations revealed that the system forms a close-packed, oriented interaction with the membrane, in which multiple PIP_2 lipids bind the canonical lipid-binding site and unique peripheral sites of the PH domain, the Arf GTPase and, unexpectedly, the Sec7 domain. We cross-validated these predictions by reconstituting the binding and kinetics of Arf and Brag2 in artificial membranes. Our coarse-grained structural model thus suggests that the high efficiency of Brag2 requires interaction with multiple lipids and a well-defined orientation on the membrane, resulting in a local PIP_2 enrichment, which has the potential to signal toward the Arf pathway.

small GTPase | lipid | guanine-nucleotide exchange factor | molecular dynamics | crystallography

The ADP ribosylation factor (Arf) small GTPases, which belong to the Ras superfamily, orchestrate a variety of regulatory functions in lipid and membrane trafficking, such as vesicular assembly, lipid modification, or lipid transport (1). In common with other members of the Ras superfamily, Arf GTPases cycle between an active GTP-bound form and an inactive GDP-bound form, via structural changes in the so-called switch 1 and switch 2 regions, which enclose the nucleotide-binding pocket. Arf GTPases also possess two additional regions that remodel during GDP/GTP alternation, including the "interswitch," which connects the switch regions, and a myristoylated amphipathic helix at their N terminus (2). Notably, the N-terminal helix tethers Arf to the membrane (3, 4) and the conformational change induced by GTP at the interswitch secures this interaction (5–7). When bound to GTP, Arf GTPases recruit diverse effectors to the membrane, and assemble membrane-bound complexes with these effectors (8). A critical step in the functional cycle of Arf GTPases is their activation by guanine-nucleotide exchange factors (ArfGEFs), which have a dual role in stimulating nucleotide exchange and localizing Arf-GTP to a membrane. Stimulation of the replacement of the tightly bound GDP by GTP is mediated by a conserved Sec7 domain, which is surrounded by an assortment of regulatory domains (9). Sec7-assisted nucleotide exchange occurs in a step-by-step manner, whereby the Sec7 domain binds to the switch 1 and switch 2 regions of Arf to remodel the interswitch and inserts an invariant glutamate into the nucleotide-binding site to displace GDP (6, 7, 10).

In metazoans, Arf GTPases are activated at the plasma membrane and on endosomes by members of three ArfGEF subfamilies: cytohesins, EFA6, and Brag/IQSEC. These ArfGEFs share a common organization in which the Sec7 domain is immediately followed by a pleckstrin homology (PH) domain that binds phosphoinositide lipids (11). In this study, we focused on the ArfGEF Brag2, (also called IQSEQ1 or ARFGEP100), which belongs to the Brag/IQSEC subfamily and comprises an N-terminal domain of about 500 residues upstream the Sec7-PH module. Members of the Brag family regulate a variety of functions, including integrin endocytosis, cell adhesion in synaptic transmission, long-term synaptic depression in neurons, muscle formation through myoblast fusion, and signaling by the EGF receptor (12). Mutations in the ArfGEF Brag1 are associated with X-chromosome–linked intellectual disability (13), and Brag2 is involved in breast cancer (14) and uveal melanoma (15). The properties of the membrane-binding PH domain in Brag2 are different from those of related Arf-specific GEFs (16). Brag2 is highly active in the absence

Significance

Small GTPases and their regulators require association to membranes to propagate actions in the cell, but our understanding of how the membrane exerts its effects has remained fragmentary. Here, we combined X-ray crystallography, coarse-grained molecular dynamics, and experimental reconstitution of the lipidated ADP ribosylation factor (Arf) GTPase and its guanine-nucleotide exchange factor, Brag2, in artificial membranes to study how this system functions on membranes. Our results reveal that the Arf/Brag2 complex interacts with multiple PIP_2 lipids, resulting in a well-defined orientation in close apposition to the membrane that explains the exceptional efficiency of activation of Arf by Brag2. Our coarse-grained model provides a structural framework to understand the assembly of Arf GTPases complexes with regulators and effectors at the surface of membranes.

Author contributions: D.K., A.N., J.K., and J.C. designed research; D.K., A.N., and J.C. performed research; D.K., A.N., J.K., and J.C. analyzed data; and J.C. wrote the paper with input from the other authors.

The authors declare no conflict of interest.

This article is a PNAS Direct Submission.

Data deposition: The atomic coordinates and structure factors have been deposited in the Protein Data Bank, www.wwpdb.org (PDB ID codes 5NLV and 5NLY).

See Commentary on page 11266.

[1]D.K. and A.N. contributed equally to this work.

[2]To whom correspondence may be addressed. Email: kuriyan@berkeley.edu or jacqueline.cherfils@ens-paris-saclay.fr.

This article contains supporting information online at www.pnas.org/lookup/suppl/doi:10.1073/pnas.1707970114/-/DCSupplemental.

of membrane, yet the efficiency of the GEF reaction (as given by the value of k_{cat}/K_m) increases by more than 100-fold when reconstituted on phosphoinositide-containing membranes, which requires interaction with the PH domain, resulting in an efficiency that nears the diffusion-controlled limit of soluble proteins (10, 17).

The crystal structure of a Sec7-PH module of Brag2 trapped in an Arf-bound intermediate state preceding GDP dissociation showed that the PH domain interacts with both the Sec7 domain and with Arf in such a way that both Arf and Brag2 can contact the membrane simultaneously (10). The linker between the Sec7 and PH domain packs against the PH domain and expands its membrane-interacting face by a loop that bears several positively charged residues. This loop is positioned near the canonical binding region of the PH domain, but its structure could not be resolved in our previous studies. Another feature of the Brag2 PH domain is the replacement of a conserved lysine residue in the canonical lipid-binding pocket by a glutamate (Glu639). In cytohesins, mutation of this lysine to alanine abolishes activity (18), but the presence of a glutamate at this position in Brag2 does not affect activity (10, 17).

The molecular detail by which the membrane exerts its effect on the efficiency of Brag2 has remained unclear because the underlying structural and thermodynamic parameters are difficult to observe experimentally. Molecular dynamics (MD) simulations offer a possible means toward understanding the origin of these effects, but all-atom MD simulations of membrane-bound proteins systems are computationally very demanding. Coarse-grained MD simulations, in which groups of atoms are combined into a single bead (19, 20), offer about a two or three order-of-magnitude increase in simulation speed at the cost of reduced structural detail, and they have proved their relevance in exploring elusive structural, dynamical, and biophysical determinants of complex membrane systems (21). Notably, coarse-grained MD simulations have provided important insights into the interaction of PH domains (22–25), and other membrane-binding domains (26–29) with membranes.

Here, we combined X-ray crystallography, coarse-grained MD simulations, and experimental reconstitution of Arf and Brag2 in artificial membranes to study the mechanism of association of Brag2 with membranes, and how its efficiency is enhanced in such an environment. We report the high-resolution crystal structure of the unbound Sec7-PH module of Brag2, which establishes that both the lipid-binding site in the PH domain and the Arf-binding site in the Sec7 domain are constitutively accessible for interactions. This structure was then used for two sets of coarse-grained MD simulations with a lipid bilayer containing phosphatidylinositol bisphosphate (PIP_2) lipids: one with unbound Brag2 and one with Brag2 complexed with myristoylated Arf1. Analyses of these simulations predict that the Arf/Brag2 complex forms multivalent interactions with the bilayer through Arf, the Sec7 domain, and the PH domain, and that these interactions lead to the formation of PIP_2-rich regions in the bilayer in the vicinity of the complex. Reconstitution of the GEF activity of Brag2 and Brag2 mutants toward myristoylated Arf in liposomes validates the structural model derived from the coarse-grained MD simulations. Our results reveal that the Arf/ArfGEF complex forms close-packed, multivalent interactions with the bilayer that result in high GEF efficiency and provides a structural framework to model the assembly of Arf GTPases complexes with regulators and effectors at the surface of membranes.

Results

Crystal Structure of the Unbound Sec7-PH Module of Brag2. We determined the crystal structure of the Sec7-PH module of human Brag2 (residues 390–763; denoted Brag2 hereafter) in two crystal forms at 2.4 Å (space group $C2_1$, one molecule in the asymmetric unit) and 2.0 Å resolution (space group $P2_12_12_1$, two molecules in the asymmetric unit), yielding three crystallographically independent copies of the protein (Fig. S1*A* and Table S1). The Sec7 and PH domains form a large intramolecular interface in all molecules, in a manner that leaves the Arf-binding site in the Sec7 domain and the canonical lipid-binding site in the PH domain fully accessible (Fig. 1*A*). Comparison of Arf-bound (10) and -unbound Brag2 shows that the interface between the two domains is essentially invariant (Fig. S1*B*), indicating that this segment of Brag2 is constitutively active and does not require a regulated displacement of the PH domain to either bind Arf GTPases or to bind to membranes. This is in striking contrast to cytohesin ArfGEFs, in which the Arf-binding site on the Sec7 domain is occluded by the PH domain and adjacent peptide segments (30) and binding of Arf-GTP is required for the release of autoinhibition (31).

Comparison of the three independent copies of Brag2 highlights significant flexibility within the Sec7 domain between the N-terminal subdomain, which bears the interface with the PH domain, and the C-terminal subdomain, which carries the Arf-binding site (Fig. 1*B*). The electron density was less well defined at helix α3, which is located at the interface between these two subdomains; this suggests that it may constitute the hinge that supports intradomain flexibility (Fig. 1*B*). Crystallographic analyses of intermediates of the exchange reaction showed that Arf rotates with respect to the Sec7 domain as the nucleotide-exchange reaction proceeds (6, 7); since the PH domain has a fixed position with respect to the Sec7 domain in Brag2, its interface with Arf should vary as Arf rotates. The flexibility of the Sec7 domain may compensate for this rotation to keep the perturbation of the Arf/PH domain interface minimal. Internal flexibility of the Sec7 domain has been observed in isolated Sec7 domains from other ArfGEF subfamilies (32). We propose that it reflects a general plasticity in Sec7 domains that is needed to accommodate changes in the contacts of Arf GTPases with adjacent domains during the exchange reaction.

The overall conformation of the PH domain is essentially identical between unbound and Arf-bound Brag2, but our new structures fully resolve the conformation of the linker between the Sec7 and PH domain. Notably, the structures show that the loop from residues 610–622 in the linker, which was not defined in the Arf-GDP/Brag2 crystal structure, expands the membrane-facing surface of the PH domain such that 10 positively charged residues are positioned for potential interaction with the bilayer (Fig. 1*C* and Fig. S1*C*). We conclude from these observations that Brag2 is constitutively active, through a structurally invariant interface between the Sec7 and PH domains, and that it displays a large positively charged, membrane-facing surface contributed by the linker and the PH domain.

Coarse-Grained MD Simulations of Brag2 with a PIP_2-Containing Lipid Bilayer. We developed a coarse-grained model for investigation of the interaction of Brag2 with the lipid bilayer, using the crystal structure of unbound Brag2. We selected an anionic lipid content of 15% phosphatidyl serine (PS) and 2% PIP_2 for coarse-grained

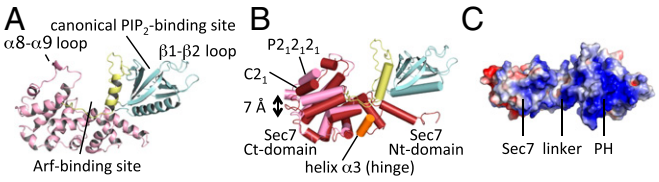

Fig. 1. Crystallographic analysis of uncomplexed Brag2. (*A*) Structure of unbound Brag2. Regions discussed in the text are indicated. The Sec7 domain is in pink, the linker in yellow, and the PH domain in blue. The same color scheme is used in all figures. (*B*) Overlay of Brag2 from $P2_12_12_1$ space group (light pink) and $C2_1$ space group (dark pink), showing the flexibility of the Sec7 C-terminal subdomain. The flexible hinge region is in orange. The orientation is as in *A*. (*C*) Electrostatic potential surface of unbound Brag2. The view is rotated by 90° with respect to *A*.

MD simulations, which approximates lipid compositions that gave strong binding and high GEF activity using liposomes (10, 17). We ran four simulations, each of which used a lipid bilayer with a cross-sectional area of 200 Å^2, in which only the layer facing the protein contained anionic lipids. The simulations were run with periodic boundary conditions to mimic an unbounded membrane. Each simulation was begun by positioning the protein near the bilayer, with the lipid-binding face of the PH domain facing toward the membrane. Each simulation was carried out for a nominal integration time of 1 μs. Note that the coarse-grained model results in lower effective friction coefficients and decreased solvent viscosity compared with all-atom models, and so the range of motions seen in a coarse-grained MD simulation over a certain timescale is much greater than that seen in an all-atom simulation extending for the same timescale (20).

In all four simulations, the Brag2 protein moves toward the membrane and engages lipids within the bilayer (Fig. 2 *A* and *B* and Fig. S2 and Movie S1). In three of the four simulations, the PH domain encountered a PIP_2 lipid almost immediately, and remained bound to it for the remainder of the simulation. In all of the simulations, once the PH domain engages the membrane, multiple residues in the PH domain form interactions with PIP_2 lipids in the membrane, leading to enhancement of the local PIP_2 density in the vicinity of the PH domain (Fig. 2 *A* and *B*). We considered the average number of interactions protein residues form with PIP_2 lipids, averaged over the simulation time (Fig. 2 *C* and *D*). Residues involved in PIP_2-binding are located in the canonical lipid-binding site (e.g., Arg654, Lys667, and Arg681), the peripheral regions in the PH domain (e.g., Lys645, Lys648, Lys671, Lys672, and Lys673), and the linker unique to BRAG family members (e.g., Lys610 and Lys611) (Fig. 2*D*; see also Fig. S1*C*). The canonical lipid-binding site of the PH domain in Brag2 has an unusual glutamate residue (Glu639) in strand β1 in place of an otherwise conserved lysine residue. The lysine residue is critical for PIP_2 binding in canonical PH domains, such as cytohesins (18, 33), leaving open the question of whether the PH domain of Brag2 bound to PIP_2 lipids at the canonical site. The coarse-grained MD simulations suggest that the presence of this glutamate in the Brag2 PH domain does not exclude PIP_2 from binding to the canonical phosphoinositide-binding site. A peripheral PIP_2-binding site is observed in loop β3-β4. Alternative PIP_2-binding sites that have been observed on the outer face of the β1-β2 strands in some PH domains (34, 35) are devoid of contacts with PIP_2 lipids in our simulations. Residues in the linker form more transient interactions with PIP_2 lipids, as indicated by the lower number of time-averaged interactions occurring in this region. Unexpectedly, we observed that the loop connecting α8-α9 in the Sec7 domain, which is located next to the Arf-binding site, interacts with PIP_2 lipids (Fig. 2*C*), raising the intriguing possibility that the contribution of membranes to the GEF reaction may not be solely mediated by the PH domain.

Taken together, coarse-grained MD simulations suggest that Brag2 interacts with PIP_2-containing membranes in a manner that involves multiple PIP_2-binding sites, located on the PH, linker, and Sec7 domains. Furthermore, these simulations identify a unique phosphoinositide-binding surface in the PH domain of Brag2, which is comprised of the phosphoinositide-binding site found in canonical PH domains, combined with peripheral sites that differ from alternative sites seen in other PH domains.

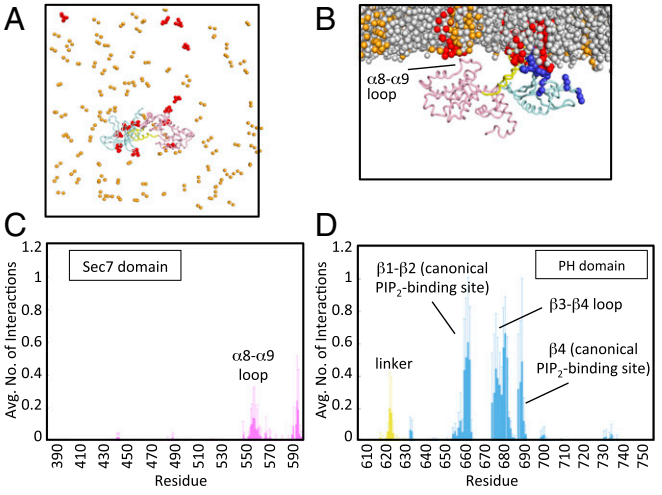

Fig. 2. Coarse-grained MD simulations of Brag2 on a membrane showing multiple PIP_2 lipid-binding sites. (*A*) Coarse-grained MD simulation of Brag2 on a membrane bilayer containing PIP_2 lipids at the end of the simulation, for one run. Multiple PIP_2s bind to the protein at various interaction sites at the end of the simulation. The PC lipids and the tails of the PS and PIP_2 lipids are not shown for clarity. (*B*) Close-up of Brag2 at the end of the simulation run, for one run. The protein binds primarily to PIP_2 molecules in the membrane at multiple binding sites. The view is rotated by 90° with respect to *A*. (*C*) Time-averaged number of interactions between Sec7 domain residues and PIP_2 lipids. The *Inset* shows a close-up of the interactions of the residues in the α8-α9 loop. Additional interactions are also seen in the loop between the Sec7 domain and the linker (residues 580–599). (*D*) Time-averaged number of interactions between residues of the linker and the PH domain, and PIP_2 lipids. See Fig. 1*A* and Fig. S1*C* for the localization of the structural elements bearing these residues. Positively charged residues (lysines and arginines) are in dark blue. PIP_2 lipids are in red; PS lipids are in orange; PC lipids are in gray.

Coarse-Grained MD Simulations of Brag2 Complexed with Myristoylated Arf on PIP_2-Containing Membranes. Next, we used coarse-grained MD simulations to investigate the interaction of the Arf/Brag2 complex with a PIP_2-containing model membrane. Normally, Arf would first engage with the membrane in a GDP-bound state, via the myristoyl moiety, followed by an encounter with Brag2 and displacement of the nucleotide. In this study, we used a model of Brag2 already complexed to Arf to study how the Arf/Brag2 complex interacts with the membrane. We selected the intermediate in which Brag2 is bound to nucleotide-free Arf, because GTPases and GEFs have the highest affinity for each other in that state (36) and the conformation of nucleotide-free Arf is competent for membrane attachment (6). Structural information for building the model of nucleotide-free myristoylated human Arf1 bound to Brag2 (hereafter referred to as ^{myr}Arf/Brag2) was derived from the structures of unbound Brag2 (present study), Arf-GDP–bound Brag2 (10), the complex of nucleotide-free Arf with the Sec7 domain of yeast Gea2 (6), and the NMR structure of myristoylated yeast Arf-GTP (4) (Fig. S3*A*). The resulting model was energy-minimized to remove local steric conflicts before it was converted into the coarse-grained model for MD simulations. An important feature is that the myristoylated N-terminal helix is readily available for interaction with the membrane in the starting conformation. We note that the set-up of our MD system, in which the GTPase/GEF complex is preformed, does not allow us to investigate the order in which discrete binding events take place. As before, the protein complex was placed above the anionic face of the membrane, with the phosphoinositide-binding region of the PH domain facing the membrane.

We ran five simulations of the ^{myr}Arf/Brag2 complex with a PIP_2-containing membrane. Long-term, stable interactions between the protein complex and the membrane occurred in four simulations (Fig. 3*A* and Fig. S4 and Movie S2). In a fifth simulation, the protein complex explored the solvent space above the membrane. This simulation was not considered in the subsequent analysis. In three of the remaining four coarse-grained MD simulations, the myristate moiety inserts into the membrane with the N-terminal helix of Arf lying parallel to the plane of the

membrane, which is consistent with NMR observations (reviewed in ref. 16).

As observed for unbound Brag2, the complex forms interactions with multiple PIP_2 lipids, and here these lipids bind to both Arf and Brag2 (Fig. 3*A* and Figs. S3*B* and S4). The Sec7, linker, and PH domains of complexed Brag2 recapitulate most of the interactions with PIP_2 lipids that were observed in the simulations of the uncomplexed protein, including interactions located in the canonical lipid-binding site and loop β3-β4 in the PH domain, the loop in the linker, and the α8-α9 loop of the Sec7 domain (Fig. 3 *B* and *C*). We note that transient interactions of positively charged residues in the loop that connects the Sec7 domain to the linker (residues 584–590) that formed with PIP_2 lipids in unbound Brag2 are disfavored when ^{myr}Arf1 is bound to Brag2, probably due to more favorable interactions provided by Arf1 itself. On the Arf side, unexpected contacts with the bilayer were observed for membrane-facing regions in Arf, notably at the tip of the interswitch (Fig. 3*D*). This region is a major determinant of the activating conformational switch, which functions as a "push button" during GTP exchange and becomes exposed early during the exchange reaction (2). This interaction suggests that the interswitch contributes toward determining the orientation of Arf on the membrane, in addition to the myristoylated N-terminal helix. Altogether, the coarse-grained MD simulations predict a structural model of the ^{myr}Arf/Brag2 complex in which the small GTPase and the GEF engage multiple lipids to establish an oriented, close-packed interface with the membrane bilayer.

Contribution of the Lipid Bilayer to Brag2 Efficiency. The coarse-grained MD simulations suggest that the high efficiency of Brag2 on a PIP_2-containing bilayer is not merely due to its colocalization with Arf, but also requires interactions of its PH, linker, and Sec7 domains with several PIP_2 lipids. We assessed these predictions by mutagenesis, membrane-binding experiments, and fluorescence-based GEF kinetics. First, we assessed whether colocalization of Brag2 and Arf is the sole contribution of liposomes by reconstituting the activation of ^{myr}Arf1 by Brag2 in two different set-ups: one in which liposomes contained neutral and NiNTA lipids to tether Brag2 by a 6-His tag in a nonspecific manner; the other in which liposomes contained PIP_2 and PS to recruit Brag2 by specific interactions. While Brag2 was entirely recruited to liposomes in both set-ups (Fig. 4*A*), it was four times less active on Ni lipid-containing liposomes, suggesting that specific interactions leading to optimal orientation are necessary for full activity (Fig. 4*B*).

Next, we analyzed the prediction that the interaction of Brag2 with the bilayer requires contacts with several PIP_2 lipids. We used a fluorescence-based thermal shift assay to determine the affinity of Brag2 to PIP_2-C4, a soluble analog of PIP_2 that carries the phosphoinositide head-group and a 4-carbon acyl chain. We found that Brag2 binds PIP_2-C4 with low affinity (>100 μM) (Fig. 4*C*), indicating that its strong interaction with the PIP_2-containing bilayer cannot be accounted for by a strong interaction with an individual PIP_2 lipid. Analysis of the fraction of protein bound to liposomes as a function of the concentration of PIP_2 in the bilayer can be used to assess whether lipids cooperate to promote membrane association (37). We measured the recruitment of Brag2 to liposomes containing increasing concentrations of PIP_2 as the sole anionic lipid, using a stringent liposome flotation assay (Fig. 4*D*). We found that Brag2 binds PIP_2 lipids in a positively cooperative manner, providing experimental support to the

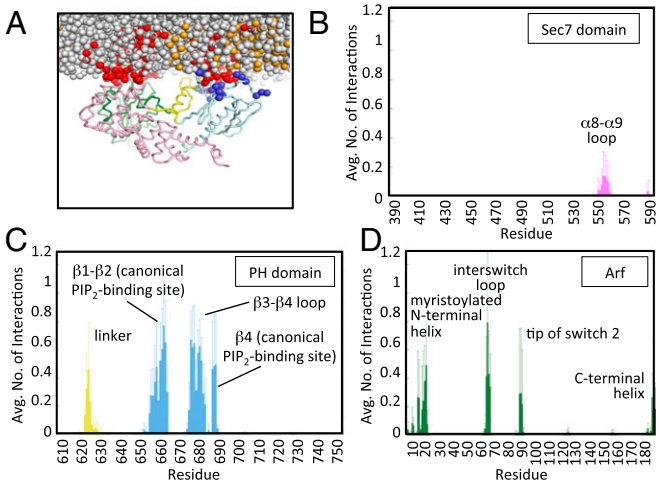

Fig. 3. Coarse-grained MD simulations of ^{myr}Arf/Brag2 on a membrane showing multiple PIP_2 lipid-binding sites. (*A*) Close-up of ^{myr}Arf/Brag2 at the end of the simulation run, for one run. Both ^{myr}Arf and Brag2 bind primarily to PIP_2 molecules in the membrane at multiple binding sites. (*B*) Time-averaged number of interactions between Sec7 domain residues and PIP_2 lipids. (*C*) Time-averaged number of interactions between the linker and PH domain residues of Brag2 and PIP_2 lipids. (*D*) Time-averaged number of interactions between Arf residues and PIP_2 lipids. Color-coding for Brag2 and lipids is as in Figs. 1 and 2. Arf is in green.

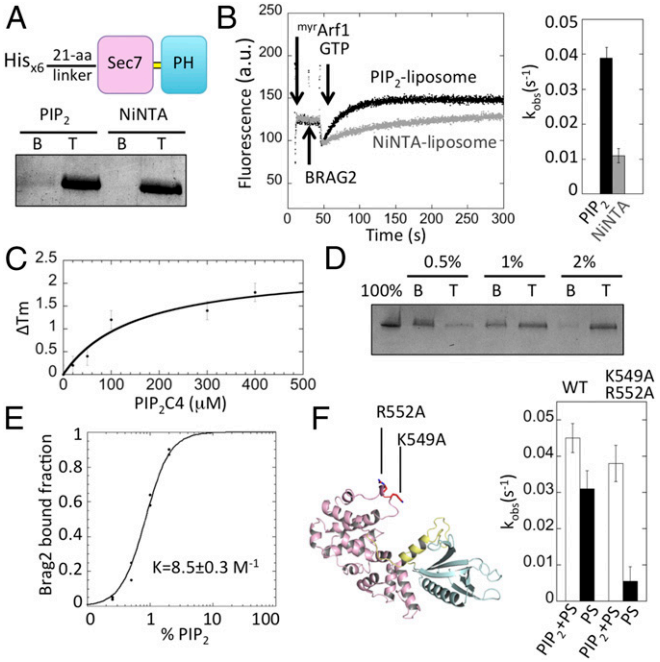

Fig. 4. Interaction of Brag2 with PIP_2 and PIP_2-containing membranes. (*A*) Flotation analysis of the interaction of Brag2 with liposomes. The His-tagged construct used in this experiment is depicted. Liposomes contained either PIP_2 or NiNTA lipids. B, bottom fraction, containing unbound proteins; T, top fraction, containing liposome-bound proteins. (*B*) Fluorescence kinetics trace showing the GEF activity of Brag2 (2 nM) toward myristoylated Arf1 (0.4 μM) in the presence of 100 μM PIP_2 liposomes (black) or NiNTA liposomes (gray). The histogram shows the corresponding k_{obs} values. (*C*) Analysis of binding of Brag2 to PIP_2-C4 using a thermal shift assay. (*D*) Liposome flotation analysis of the interaction of Brag2 with liposomes containing increasing PIP_2 concentrations. (*E*) Fraction of liposome-bound Brag2 as a function of PIP_2 concentration. The Hill plot analysis shown in Fig. S5*A* indicates that PIP_2 lipids bind to Brag2 in a positively cooperative manner. (*F*) Analysis of the GEF efficiency on membranes of Brag2 carrying mutations in the Sec7 domain. Liposomes contained either PIP_2 or PS as a source of anionic lipids. The position of the mutations in the Sec7 domain is shown. Composition of liposomes is given in Table S2.

coarse-grained MD prediction that it binds to multiple PIP_2 lipids (Fig. 4*E* and Fig. S5*A*). We note that a small fraction of Brag2 remains unbound to liposomes that contain PIP_2 as the sole source of negatively charged lipids, while Brag2 is entirely bound to liposomes that contain both PS and PIP_2 (Fig. S5*B*). Surprisingly, PIP_2-only liposomes support a higher GEF activity than PIP_2-PS liposomes (Fig. S5*C*). These observations suggest that while PS increases the binding of Brag2 to PIP_2-containing membranes, optimal activity of Brag2 is favored by an increased ability to dissociate from membranes.

Finally, we assessed the predicted contribution of the Sec7 domain of Brag2 to its interaction with the lipid bilayer. A role for Sec7 domains in binding membranes has not been envisioned before because their activity is not enhanced by membranes (10, 38) and the Sec7 domain of Brag2 binds poorly, if at all, to liposomes (10). We produced a Brag2 double mutant in which K549 and R552 in the α8-α9 loop of the Sec7 domain were replaced by alanines, which should have impaired activity on anionic membranes based on the CG-MD model. The double mutation does not affect the GEF efficiency in solution, indicating that the mutant is well folded and that the site of the mutation is not directly involved in the GEF reaction (Fig. S5*D*). Remarkably, whereas Brag2 was highly active on liposomes containing either both PIP_2 and PS or PS alone as a source of anionic lipids, the double mutant was active on PIP_2-PS liposomes but was severely impaired on PS-liposomes (Fig. 4*F*). Thus, the mutant has defects in its regulation by membranes that can be overcome by PIP_2 lipids, probably through interactions of its linker and PH domains with PIP_2 lipids that cannot be established properly by PS alone. These data indicate that the positively charged loop in the Sec7 domain is involved in the recognition of anionic membranes, and that this interaction contributes to the GEF efficiency. Taken together, these data support the coarse-grained MD model of ^{myr}Arf/Brag2 bound to a PIP_2-containing bilayer in which it forms an oriented complex that interacts with multiple PIP_2 lipids.

Discussion

In this study, we devised and cross-validated a coarse-grained structural model of ^{myr}Arf/Brag2 complex bound to a PIP_2-containing bilayer by combining crystallography, coarse-grained MD simulations, and reconstitution of small GTPase and GEF in artificial membranes. It is unique in that coarse-grained MD simulations have been used to model a membrane-attached GTPase/regulator complex, and it reveals elusive aspects of the mechanism of activation of Arf GTPases with implications for their functions.

The structural model of the bilayer-associated ^{myr}Arf/Brag2 complex features several layers of interactions, including a rigid intramolecular interaction between the Sec7 and PH domains of the GEF, adjustable protein–protein interactions between Arf and both domains of the GEF, and interactions of the complex with multiple lipids. PIP_2 lipids interact with the canonical lipid-binding site of the PH domain, a peripheral site in the PH domain, a positively charged loop in the linker, a loop in the Sec7 domain, the myristoylated N-terminal helix, and loop of the interswitch in Arf. While the contribution of the PH domain and the linker to the regulation of the exchange reaction on PIP_2-containing membranes had been reported before (10, 17), the contribution of the Sec7 domain to defining the geometry of the membrane-attached complex was not anticipated. An important finding is that the lipidated Arf/Brag2 complex is apposed closely to the membrane by these multiple contacts with lipids, which constrains both its geometry and orientation. We propose that the exceptional efficiency of the activation of Arf by Brag2 on membranes results from the integration of these optimized intramolecular, protein–protein and protein–membrane interactions. Whether and how other elements in the N terminus of the protein regulate this constitutively active module will have to be investigated. It is interesting to note that the interaction of the interswitch of Arf with membranes results from the action of GEF, which promotes the toggle of the interswitch to its exposed conformation; the strength of the interaction of Arf with membranes should therefore strengthen as the exchange reaction proceeds. In practical terms, the close-packed arrangement of the Arf/Brag2/membrane system leaves little space to accommodate the large tags used for detection in cellular assays, and the presence of tags may therefore impair this arrangement. This explains why domain tags fused to yeast Arf GTPases affect their functions (39). We also observed that the myristoylated N-terminal helix of Arf is close to the Sec7 domain in the membrane-attached complex; accordingly, the Sec7 domain may perceive conformational information from this helix, such as its orientation with respect to the GTPase core. This raises the interesting possibility that this pivotal regulatory element of Arf GTPases, which is where the sequences of the five Arf isoforms diverge the most, conveys specificity information that can be monitored by the GEFs. More generally, our analysis points to a common organization of protein complexes assembled by Arf GTPases, in which Arf GTPases position their regulators and effectors such that they are poised to form multiple and oriented interactions with the lipid bilayer. A powerful approach to testing the predictions of our model will be to determine the orientation of Brag2 on the membrane by NMR, and delineate how the orientation is correlated with the engagement of phosphatidyl inositol lipids, as demonstrated recently for Ras (40). In the future, it will also be important to test these findings in the context of the cell, for example by studying the effect of mutations in the Sec7 and linker domains of Brag2 on the level of Arf activation.

Our analysis also provides insight into the dynamics of PIP_2 lipids located in the membrane bilayer in the vicinity of the Arf/Brag2 complex, with potential implications for Arf functions. In the coarse-grained simulations, the complex interacts with multiple lipids, most of which exchange dynamically in the course of the simulation, and this interaction with multiple lipids is supported by membrane-binding experiments. In effect, this leads to enrichment of PIP_2 lipids in the vicinity of the complex, an effect reminiscent of lipid clustering that has been observed in experimental studies using model membranes and cellular assays, and in MD simulations of PH and other PIP_2-binding domains (41, 42). At the level of the GEF reaction, PIP_2 enrichment could contribute a positive feedback effect by strengthening the interaction of the complex with the membrane or it could delimit the membrane domain where Brag2 is located and produces Arf-GTP, thereby modulating the amplitude and shape of the Arf-GTP signal generated by Brag2. Consistent with this prediction, we observed that Brag2 was more active on liposomes to which it bound more weakly than on liposomes where it was recruited strongly, highlighting that the spacio-temporal activity of Brag2, and probably of any GEF, depends on an exquisite balance between the strength of membrane binding and the GEF efficiency. PIP_2 enrichment could also be perceived by components of pathways downstream of Arf, possibly even without their interacting directly with activated Arf. This could be especially relevant to the lipid-modifying enzymes phospholipase D, which breaks down PIP_2 to generate phosphatidic acid, and PI(4)P-5 kinase, which uses PI(4)P to synthesize PIP_2, both of which are downstream effectors of Arf at the plasma membrane. Arf and PIP_2 lipids are known to synergize to activate phospholipase D, while phosphatidic acid produced by phospholipase D synergizes with Arf to activate PI(4)P-5 kinase, with the potential for an "explosive feedforward loop" (43) in the production of PIP_2. Our study highlights that Arf and Brag2 play an active role in organizing the pool of PIP_2 lipids that are used as activators or substrates by these Arf effectors. Whether or not this effect suffices to account for the role of Arf in the regulation of phospholipase D and PI(4)P-5 kinase, the net balance of PIP_2 production is likely to be tuned by combination of direct enzymatic contributions and the indirect contributions of Arf and its GEFs.

In conclusion, our analysis identifies geometric determinants and multiple lipid interactions that determine the amplitude and regulation of the activation of Arf by its GEFs. We propose that the formation of PIP_2-rich regions by Arf and Brag2 contributes to propagating signals in coordination with Arf activation. Given that the negative regulators (GAPs) and effectors also interact with membrane attached Arf-GTP, our study should provide a valuable framework to model the interaction of these complexes and envision direct and indirect regulation by signaling phosphoinositides. More generally, it points to the functional relationship between the geometry of association of small GTPases, regulators, and effectors with membranes and their signaling output, as recently illustrated for lipidated K-Ras (44).

Materials and Methods

Proteins, crystallization and structure determination, thermal shift assay, liposome-binding assay, nucleotide-exchange kinetics, and coarse-grained MD simulations are described in *SI Materials and Methods*.

ACKNOWLEDGMENTS. We thank the scientific staff at the PROXIMA-1 and PROXIMA-2 (SOLEIL) and ID23-2 (European Synchrotron Radiation Facility) X-ray diffraction beamlines for making the beamlines available to us and for their help and excellent advice; and Mahel Zeghouf (CNRS and Ecole Normale Supérieure Paris-Saclay) for discussions. This work was supported by grants from the Institut National du Cancer and the Fondation pour la Recherche Médicale, and by a Visiting Professorship award from the Miller Institute for Basic Research in Science, University of California, Berkeley (to J.C.).

1. Donaldson JG, Jackson CL (2011) ARF family G proteins and their regulators: Roles in membrane transport, development and disease. *Nat Rev Mol Cell Biol* 12:362–375.
2. Pasqualato S, Renault L, Cherfils J (2002) Arf, Arl, Arp and Sar proteins: A family of GTP-binding proteins with a structural device for 'front-back' communication. *EMBO Rep* 3:1035–1041.
3. Antonny B, Beraud-Dufour S, Chardin P, Chabre M (1997) N-terminal hydrophobic residues of the G-protein ADP-ribosylation factor-1 insert into membrane phospholipids upon GDP to GTP exchange. *Biochemistry* 36:4675–4684.
4. Liu Y, Kahn RA, Prestegard JH (2010) Dynamic structure of membrane-anchored Arf*GTP. *Nat Struct Mol Biol* 17:876–881.
5. Amor JC, Harrison DH, Kahn RA, Ringe D (1994) Structure of the human ADP-ribosylation factor 1 complexed with GDP. *Nature* 372:704–708.
6. Goldberg J (1998) Structural basis for activation of ARF GTPase: Mechanisms of guanine nucleotide exchange and GTP-myristoyl switching. *Cell* 95:237–248.
7. Renault L, Guibert B, Cherfils J (2003) Structural snapshots of the mechanism and inhibition of a guanine nucleotide exchange factor. *Nature* 426:525–530.
8. Cherfils J (2014) Arf GTPases and their effectors: Assembling multivalent membrane-binding platforms. *Curr Opin Struct Biol* 29:67–76.
9. Casanova JE (2007) Regulation of Arf activation: The Sec7 family of guanine nucleotide exchange factors. *Traffic* 8:1476–1485.
10. Aizel K, et al. (2013) Integrated conformational and lipid-sensing regulation of endosomal ArfGEF BRAG2. *PLoS Biol* 11:e1001652.
11. Lemmon MA (2008) Membrane recognition by phospholipid-binding domains. *Nat Rev Mol Cell Biol* 9:99–111.
12. D'Souza RS, Casanova JE (2016) The BRAG/IQSec family of Arf GEFs. *Small GTPases* 7:257–264.
13. Shoubridge C, et al. (2010) Mutations in the guanine nucleotide exchange factor gene IQSEC2 cause nonsyndromic intellectual disability. *Nat Genet* 42:486–488.
14. Morishige M, et al. (2008) GEP100 links epidermal growth factor receptor signalling to Arf6 activation to induce breast cancer invasion. *Nat Cell Biol* 10:85–92.
15. Yoo JH, et al. (2016) ARF6 is an actionable node that orchestrates oncogenic GNAQ signaling in uveal melanoma. *Cancer Cell* 29:889–904.
16. Nawrotek A, Zeghouf M, Cherfils J (2016) Allosteric regulation of Arf GTPases and their GEFs at the membrane interface. *Small GTPases* 7:283–296.
17. Jian X, Gruschus JM, Sztul E, Randazzo PA (2012) The pleckstrin homology (PH) domain of the Arf exchange factor Brag2 is an allosteric binding site. *J Biol Chem* 287:24273–24283.
18. Stalder D, et al. (2011) Kinetic studies of the Arf activator Arno on model membranes in the presence of Arf effectors suggest control by a positive feedback loop. *J Biol Chem* 286:3873–3883.
19. Marrink SJ, Risselada HJ, Yefimov S, Tieleman DP, de Vries AH (2007) The MARTINI force field: Coarse grained model for biomolecular simulations. *J Phys Chem B* 111:7812–7824.
20. Ingólfsson HI, et al. (2014) The power of coarse graining in biomolecular simulations. *Wiley Interdiscip Rev Comput Mol Sci* 4:225–248.
21. Ingólfsson HI, Arnarez C, Periole X, Marrink SJ (2016) Computational 'microscopy' of cellular membranes. *J Cell Sci* 129:257–268.
22. Lumb CN, Sansom MS (2012) Finding a needle in a haystack: The role of electrostatics in target lipid recognition by PH domains. *PLOS Comput Biol* 8:e1002617.
23. Lai CL, et al. (2013) Molecular mechanism of membrane binding of the GRP1 PH domain. *J Mol Biol* 425:3073–3090.
24. Yamamoto E, Kalli AC, Yasuoka K, Sansom MS (2016) Interactions of pleckstrin homology domains with membranes: Adding back the bilayer via high-throughput molecular dynamics. *Structure* 24:1421–1431.
25. Naughton FB, Kalli AC, Sansom MS (2016) Association of peripheral membrane proteins with membranes: Free energy of binding of GRP1 PH domain with phosphatidylinositol phosphate-containing model bilayers. *J Phys Chem Lett* 7:1219–1224.
26. Janosi L, Li Z, Hancock JF, Gorfe AA (2012) Organization, dynamics, and segregation of Ras nanoclusters in membrane domains. *Proc Natl Acad Sci USA* 109:8097–8102.
27. Yu H, Schulten K (2013) Membrane sculpting by F-BAR domains studied by molecular dynamics simulations. *PLOS Comput Biol* 9:e1002892.
28. Picas L, et al. (2014) BIN1/M-Amphiphysin2 induces clustering of phosphoinositides to recruit its downstream partner dynamin. *Nat Commun* 5:5647.
29. Simunovic M, Voth GA (2015) Membrane tension controls the assembly of curvature-generating proteins. *Nat Commun* 6:7219.
30. DiNitto JP, et al. (2007) Structural basis and mechanism of autoregulation in 3-phosphoinositide-dependent Grp1 family Arf GTPase exchange factors. *Mol Cell* 28:569–583.
31. Malaby AW, van den Berg B, Lambright DG (2013) Structural basis for membrane recruitment and allosteric activation of cytohesin family Arf GTPase exchange factors. *Proc Natl Acad Sci USA* 110:14213–14218.
32. Renault L, Christova P, Guibert B, Pasqualato S, Cherfils J (2002) Mechanism of domain closure of Sec7 domains and role in BFA sensitivity. *Biochemistry* 41:3605–3612.
33. Lietzke SE, et al. (2000) Structural basis of 3-phosphoinositide recognition by pleckstrin homology domains. *Mol Cell* 6:385–394.
34. Ceccarelli DF, et al. (2007) Non-canonical interaction of phosphoinositides with pleckstrin homology domains of Tiam1 and ArhGAP9. *J Biol Chem* 282:13864–13874.
35. Jian X, et al. (2015) Molecular basis for cooperative binding of anionic phospholipids to the PH domain of the Arf GAP ASAP1. *Structure* 23:1977–1988.
36. Cherfils J, Zeghouf M (2013) Regulation of small GTPases by GEFs, GAPs, and GDIs. *Physiol Rev* 93:269–309.
37. Pérez-Lara Á, et al. (2016) PtdInsP2 and PtdSer cooperate to trap synaptotagmin-1 to the plasma membrane in the presence of calcium. *eLife* 5:e15886.
38. Padovani D, et al. (2014) EFA6 controls Arf1 and Arf6 activation through a negative feedback loop. *Proc Natl Acad Sci USA* 111:12378–12383.
39. Jian X, Cavenagh M, Gruschus JM, Randazzo PA, Kahn RA (2010) Modifications to the C-terminus of Arf1 alter cell functions and protein interactions. *Traffic* 11:732–742.
40. Mazhab-Jafari MT, et al. (2015) Oncogenic and RASopathy-associated K-RAS mutations relieve membrane-dependent occlusion of the effector-binding site. *Proc Natl Acad Sci USA* 112:6625–6630.
41. Brown JC, et al. (2016) Bidirectional regulation of synaptic transmission by BRAG1/IQSEC2 and its requirement in long-term depression. *Nat Commun* 7:11080.
42. Picas L, Gaits-Iacovoni F, Goud B (2016) The emerging role of phosphoinositide clustering in intracellular trafficking and signal transduction. *F1000 Res* 5:422.
43. Czech MP (2000) PIP2 and PIP3: Complex roles at the cell surface. *Cell* 100:603–606.
44. Zhou Y, et al. (2017) Lipid-sorting specificity encoded in K-Ras membrane anchor regulates signal output. *Cell* 168:239–251.e16.
45. McCoy AJ (2007) Solving structures of protein complexes by molecular replacement with Phaser. *Acta Crystallogr D Biol Crystallogr* 63:32–41.
46. Adams PD, et al. (2010) PHENIX: A comprehensive Python-based system for macromolecular structure solution. *Acta Crystallogr D Biol Crystallogr* 66:213–221.
47. Blanc E, et al. (2004) Refinement of severely incomplete structures with maximum likelihood in BUSTER-TNT. *Acta Crystallogr D Biol Crystallogr* 60:2210–2221.
48. Emsley P, Cowtan K (2004) Coot: Model-building tools for molecular graphics. *Acta Crystallogr D Biol Crystallogr* 60:2126–2132.
49. Dolinsky TJ, et al. (2007) PDB2PQR: Expanding and upgrading automated preparation of biomolecular structures for molecular simulations. *Nucleic Acids Res* 35:W522–W525.
50. Case DA, et al. (2005) The Amber biomolecular simulation programs. *J Comput Chem* 26:1668–1688.
51. Monticelli L, et al. (2008) The MARTINI coarse-grained force field: Extension to proteins. *J Chem Theory Comput* 4:819–834.
52. Wassenaar TA, Ingólfsson HI, Böckmann RA, Tieleman DP, Marrink SJ (2015) Computational lipidomics with Insane: A versatile tool for generating custom membranes for molecular simulations. *J Chem Theory Comput* 11:2144–2155.
53. Bussi G, Donadio D, Parrinello M (2007) Canonical sampling through velocity rescaling. *J Chem Phys* 126:014101.
54. Berendsen HJC, Postma JPM, van Gunsteren WF, DiNola A, Haak JR (1984) Molecular dynamics with coupling to an external bath. *J Chem Phys* 81:3684–3690.
55. Parrinello M, Rahman A (1981) Polymorphic transitions in single crystals: A new molecular dynamics method. *J Appl Phys* 52:7182–7190.
56. Pronk S, et al. (2013) GROMACS 4.5: A high-throughput and highly parallel open source molecular simulation toolkit. *Bioinformatics* 29:845–854.